Experimental and Analytical Investigation on the Effectiveness of External Stiffeners on CHS T-Joints Subjected to Repeated Load

Hanan H. Eltobgy, Emad Darwish, Mohamed A. Aboshok

ABSTRACT:
Adding stiffener to Circular Hollow Section CHS connection is a common method to strength this type of connection. This manuscript investigated the effectiveness of using stiffener with CHS T-joint subjected to cyclic load. Four full scale specimens were experimentally studied under cyclic load, two specimens were unreinforced joints, and the others were reinforced with stiffener. Hysteretic curves were plotted from load displacement data and S curves were extracted from them. The failure mode, the hysteretic curves and energy dissipation of the four full-scale specimens were examined, and it was found that the integrated area within hysteretic curves of the stiffened T-joints is larger than the enclosed area of the un-stiffened specimens because chord reinforcement improved the joint bearing capacity. Finite element (FE) analysis was conducted using the ABAQUS soft package. Results obtained from Finite element models (FEM) were verified with experimental results and found in favorable agreement with experiment results. Stress distribution displayed from FEM and compared with fracture observed from experiments. FEM is extended to study the effect of external stiffeners on CHS T-Joints' capacity with different brace to chord diameter ratios β. Although external stiffeners decreased stress concentration around joints by increasing load distribution area, positive joint capacity enhanced by 10% and there was an unremarkable improvement in a negative capacity. By the end of the research, the imperial formulation for joint capacity was performed and examined by the experimental and numerical results.

Keywords - Circular Hollow Sections, Cyclic Load, Hysteretic Curve, T-joint, Stiffener, Capacity, Stress Concentration.

1 Introduction

Nowadays, using tubular structures became in several types such as steel towers, offshore and building's façade. These structure may be subjected to quasi-static load, therefore in this research, the behavior of CHS T-joints investigated under cyclic load. Literature study represented previous work conducted on CHS joints subjected to different types of static load.

Ding at al [1] represented an experimental and numerical study on CHS X-joints with stiffeners under static load. Their research was conducted on different geometric variations of brace to chord diameter ratio β, with and without stiffeners. The results showed that connection stiffeners clearly increased the tensile mechanical performance of joints and the ultimate strength enhanced with the increase in brace to chord ratio, β.

Axial compression capacity investigated of X-joints for several brace-to-chord diameter ratio β experimentally and numerically [2]. Existence of stiffener increased X-joints capacity for the studied geometry parameters. Numerically, improvement in joint capacity observed with change in size of stiffener, also empirical equation was extracted based on modified yield line model.

The work of [3] provided guidelines for proper detailing of stiffeners and their impact to joints strength as opposed to the original un stiffened joint. Their work showed enhancement in CHS X-joint capacity when change stiffener's geometry parameters (diameter, thickness and spacing). There were two outer ring stiffener surrounding chord on each side of brace location. This proposed stiffener location avoids zones of affected weld that will be suitable strengthening solution for existing joints.

Using FEM, [4] studied the change in axial strength of both the un reinforced and reinforced CHS T-joints. After carrying out validation tests, the numerical models were then used to analyze the variations in strength of differently sized stiffeners. The results showed an increase in joint strength with an increase in stiffener size. In fact, change in stiffener length has remarkable improvement in joint, unlike stiffener height has unremarkable enhancement in joint behavior.

The impact of axial compression on externally stiffened CHS T-joints through FEM and theoretical analysis was investigated by [5]. FEM was verified with nine experiment specimens. A parametric study, using FEM, was then expanded on to study the effect of external stiffeners size and joint geometry on the improvement of ultimate capacity of the joints against axial compression. Improvement in joint capacity was not noticed when stiffener thickness was more than chord thickness. However, joint capacity decreased when brace to chord diameter β increased, whereas change in stiffener length to the brace diameter η remained joint capacity almost proportional. Empirical equation was extracted to predict enhancement capacity for T-joints reinforced with stiffener.

[6] investigated the enhancement in tensile performance of CHS using external stiffening ring by changing β. In the experimental results failure modes were observed, weld failure and chord plastification. Test results also revealed enhancements in ultimate load and initial stiffness. This was exploited to create a FEM shell element capable of predicting static performance of the X-joints subjected to brace tensile load with and without external stiffening rings.

Hanan H. Eltobgy, Associate Professor, Civil Eng. Department, Faculty of Engineering, Shoubra, Benha University, Egypt. E-mail: hanan.altobgy@feng.bu.edu.eg

Emad Darwish, Lecturer, Civil Eng. Department, Faculty of Engineering, Shoubra, Benha University, Egypt. E-mail: emad.darwish@feng.bu.edu.eg

Mohamed A. Aboshok, Assistant Lecturer, Civil Eng. Department, Faculty of Engineering, Shoubra, Benha University, Egypt. E-mail: mohamed.aboshok@feng.bu.edu.eg

Material hardening should be adjusted when subjected to cyclic load, isotropic and kinematic hardening parameters should be evaluated [7]. These hardening parameters could be obtained from tensile coupon test [8], provide an acceptable material representation when subjected to cyclic load.

Present research on tubular joints extensively studied the static behavior, however the dynamic behavior of such joints was rarely investigated. Moreover, the numerical models that are able to predict the dynamic behavior of tubular joints are not well affirmed up till now. Therefore, there is a need to perform cyclic test on CHS joints and to develop proportionate dependable analytical models. This research studied the effectiveness of adding external stiffeners to CHS T-joints subjected to cyclic load. The behavior of joints was investigated through numerical and experimental studies. Results comparison conducted through joint capacity and stress distribution of joint, numerical results were in favorable agreement with experimental results. Joint capacity was calculated for different brace to chord diameter β and the fitting equation between capacity and β was extracted for reinforced and unreinforced joints.

2 Experiment Study

Experimental work was conducted to study the behavior of CHS T-joint (unreinforced and reinforced with stiffeners) subjected to cyclic load. The behavior was check through failure observation, hysteresis curve and joint capacity.

2.1 Specimens and Setup

Four specimens were selected to investigate the behavior of CHS T-joints against cyclic loads, two represents unreinforced joints (SP01 and SP02) and the others represented reinforced joint with 2-stiffeners 100*6 (SP03 & SP04). Joint component dimensions were listed in

Table 1. Coupon test was performed to define material mechanical properties, yield and ultimate strength were 326 and 460 Mpa, respectively. Specimens were fabricated and erected on laboratory frame as shown in Fig. 1.

Table 1 Experiment Specimens

Specimen No.	T-joint Type	Chord		Brace		Stiffener	
		D (mm)	T (mm)	d (mm)	T (mm)	Lst (mm)	Tst (mm)
SP01	Default	114	3	114	3		
SP02	Default	88	3	114	3		
SP03	Stiffener	114	3	114	3	100	6
SP04	Stiffener	88	3	114	3	100	6

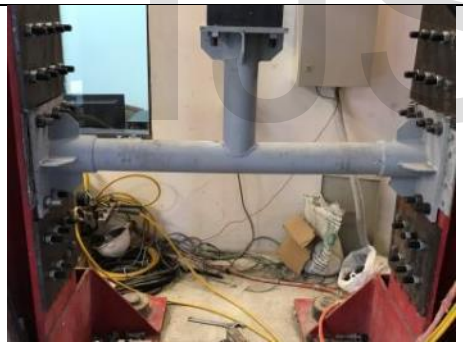

a) Test Setup for SP01

b) Test Setup for SP02

c) Test Setup for SP03

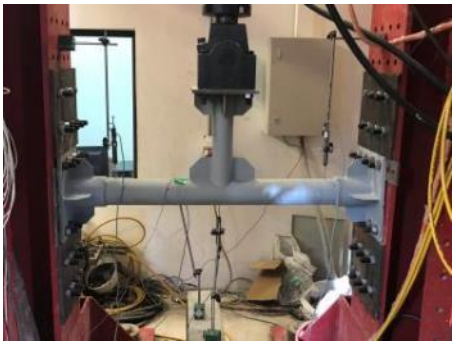

d) Test Setup for SP04

Fig. 1 Experiment Setup

Cyclic load was applied through a single ended servo-controlled actuator, that operated by load protocol based on Federal Emergency Management Agency, FEMA-461 [9]. Load protocol was governed by joint yield displacement, that was calculated from a monotonic test as indicated in

Table 2. Load displacement data was extracted through a digital data acquisition system Model DTE~500 connected to a computer.

Table 2 Load Protocol

Displacement (mm)	1.25	2.50	3.75	5.00	7.00	9.80	13.72	19.21	26.89	37.64
No. of Cycles	2	2	2	2	2	2	2	2	2	2

2.2 Failure Mode Observations

Failure mechanism has been different between tested specimens. For SP01 and SP02, test was terminated after 15 cycles and plasticity of chord around connection location governed the failure mode. Specimens with stiffeners sustained till 18 cycles and the failure mode was chord's plasticity accompanied by cutting in chord as shown in Fig. 2. Existence of stiffener did not increase initial stiffness of chord, and so max load capacity was not enhanced with great value. However, reinforced specimens can sustain more cycles and well distribute stress around connection perimeter.

e) SP01 Failure Location

f) SP02 Failure Location

c) SP03 Failure Location

d) SP04 Failure Location

Fig. 2 Failure Modes

2.3 Hysteresis Curve

Hysteresis curves were plotted from load displacement data extracted from laboratory instruments. Hysteresis curve were analyzed to obtain S curve, that resulting from identify inflection points on curve and connecting between them as shown in Fig. 3 to Fig. 6. Positive and Negative capacities (P_{u+ve} and P_{u-ve}) and displacement (Δ_y and Δ_u) could be obtained from S curve as listed in Table 3. There was a little enhancement within 10 % in joint capacity when adding stiffener to joint. Existence of stiffener increased distributed load area but was not introduce any additional stiffness to chord.

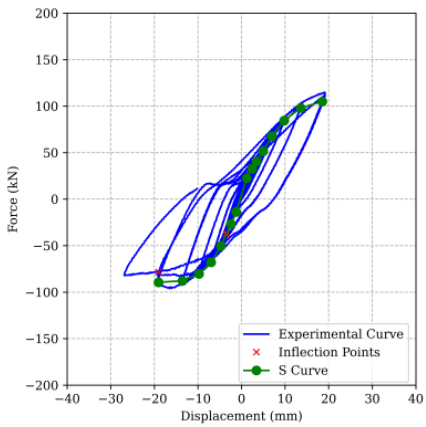

a) Hysteresis Curve and Inflection Points for SP01

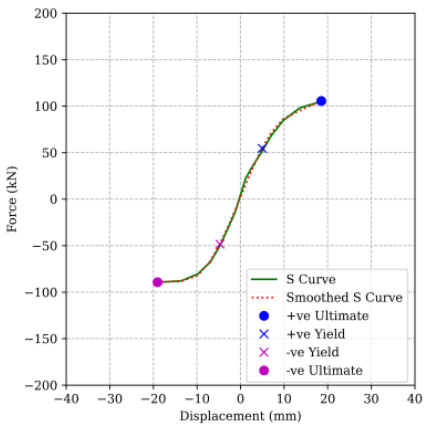

b) Smoothed S Curve for SP01

Fig. 3 Hysteresis Curve and S Curve for SP01

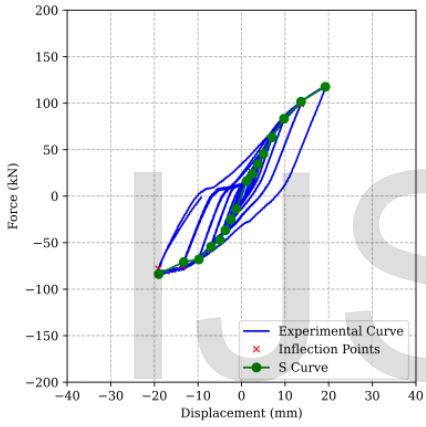

a) Hysteresis Curve and Inflection Points for SP02

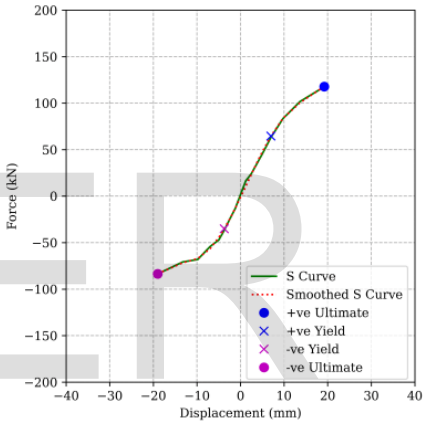

b) Smoothed S Curve for SP02

Fig. 4 Hysteresis Curve and S Curve for SP02

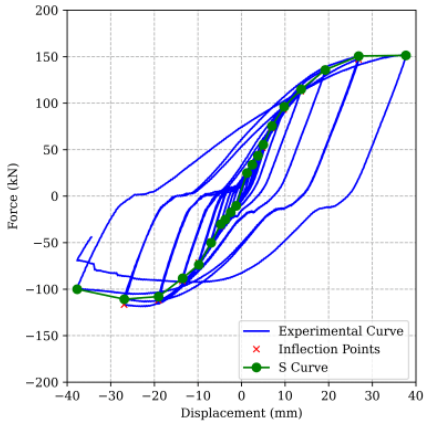

a) Hysteresis Curve and Inflection Points for SP03

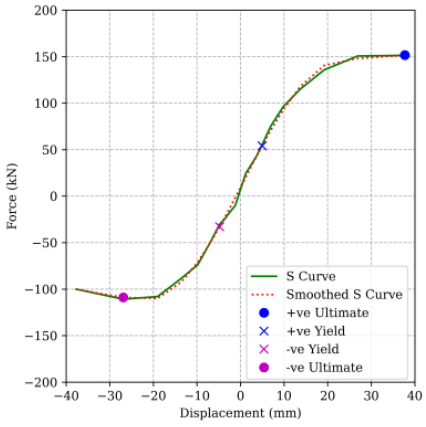

b) Smoothed S Curve for SP03

Fig. 5 Hysteresis Curve and S Curve for SP03

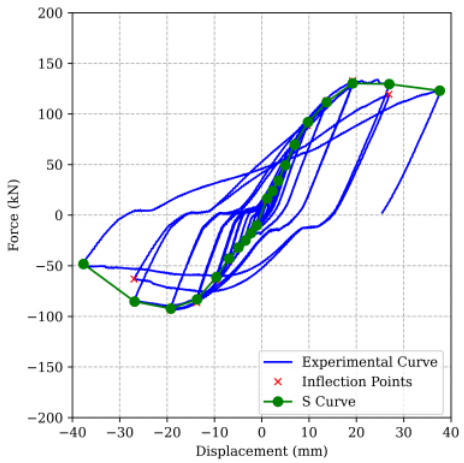

a) Hysteresis Curve and Inflection Points for SP04

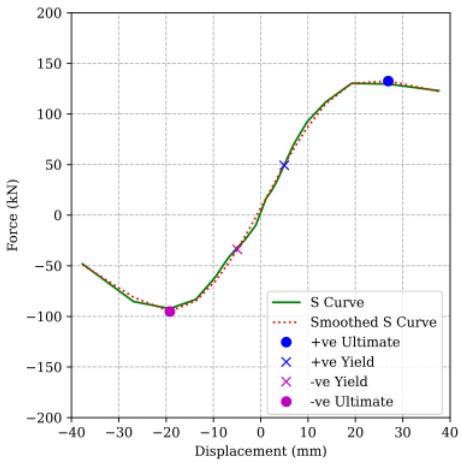

b) Smoothed S Curve for SP04

Fig. 6 Hysteresis Curve and S Curve for SP04

Table 3 Positive and Negative Capacities Extracted from S Curve

Specimen No.	Displacement				Force			
	Δ_{y+ve} (mm)	Δ_{u+ve} (mm)	Δ_{y-ve} (mm)	Δ_{u-ve} (mm)	P_{y+ve} (KN)	P_{u+ve} (KN)	P_{y-ve} (KN)	P_{u-ve} (KN)
SP01	4.98	18.52	-4.71	-19.03	54.62	105.58	-48.33	-89.23
SP02	6.99	19.21	-3.72	-19.00	64.54	117.80	-35.10	-83.53
SP03	4.97	37.69	-4.78	-26.89	54.01	151.63	-32.87	-108.91
SP04	4.96	26.92	-4.96	-19.21	49.26	132.50	-33.82	-95.15

3 Numerical Study

Finite Element Model was conducted using ABAQUS software and verified by the experimental results. Weld simulation and residual stress were ignored in FEM [10]. Comparison between experiment and numerical was achieved through hysteresis curve.

3.1 Finite Element Model (FEM)

FEM was performed through defining model input data (parts, material, boundary condition, mesh, step, and history output). Parts were modeled as 3D Solid Deformable part. Material parameters defined such as density, elastic and plastic ranges as extracted from coupon test. Material subjected to cyclic load needed to identify combined hardening parameters. A kinematic and isotropic hardening material model is adopted with properties taken from the tensile coupon tests [11]. Damage and fracture mechanisms were not applied into the FE model. General static analysis had been applied on FEM, there was a step for each amplitude in load cycle. Boundary condition at the ends is simulated with end plates to represent the experimental setup, where the end plates are restrained at bolt locations. Load was applied in model as displacement control at reference point with amplitude value in load protocol. A refined finer mesh was created at the intersection zone of connection to obtain a representative stress distribution value as shown in Fig. 7. C3D8R an 8-node linear brick, reduced integration, hourglass control mesh elements are used in ABAQUS to build the FE models, this element type provides a good mesh of hexahedral elements. Determining result parameters through history and field outputs.

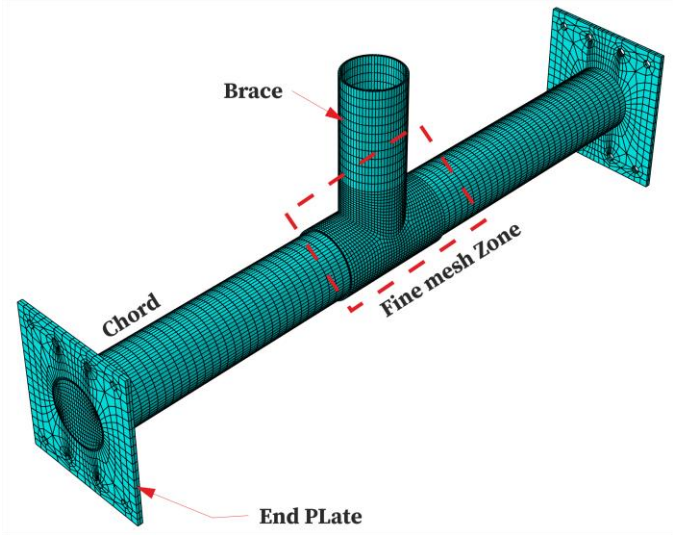

Fig. 7 FEM Geometry and Mesh

3.2 Hysteresis Curve

Load displacement curves for specimens were plotted from history output variables, manual termination is defined in FEM results since, the analysis did not obtain a fracture mechanism. Comparison was conducted between hysteresis curve for FEM in red color and experiment curve in blue, and it was noticed that the behavior of hysteresis curves was very close to each other in all tested specimens as shown in Fig. 8. S curves were extracted from hysteresis curve, yield and ultimate domains for positive and negative zones could be obtained as shown in Fig. 9. For positive zone, yield domain (Δ_{y+ve} and P_{y+ve}) located in x orange symbol and ultimate domain (Δ_{u+ve} and P_{u+ve}) plotted in dot blue symbol. Negative yield domain (Δ_{y-ve} and P_{y-ve}) determined with x green symbol, and negative ultimate domain (Δ_{u-ve} and P_{u-ve}) presented in dot red. Capacities FEM results were in a good agreement with experiment results as listed in Table 4 Capacity Comparison for Experiment and FEM

Specimen No.	Experiment		FEM		% diff of P_{u+ve}	% diff of P_{u-ve}
	P_{u+ve}	P_{u-ve}	P_{u+ve}	P_{u-ve}		
SP01	105.58	-89.23	101.13	-106.57	-4.21 %	19.43 %
SP02	117.80	-83.53	98.72	-81.79	-16.20 %	-2.08 %
SP03	151.63	-108.91	151.68	-129.95	0.03 %	19.31 %
SP04	132.50	-95.15	143.95	-95.76	8.64 %	0.64 %

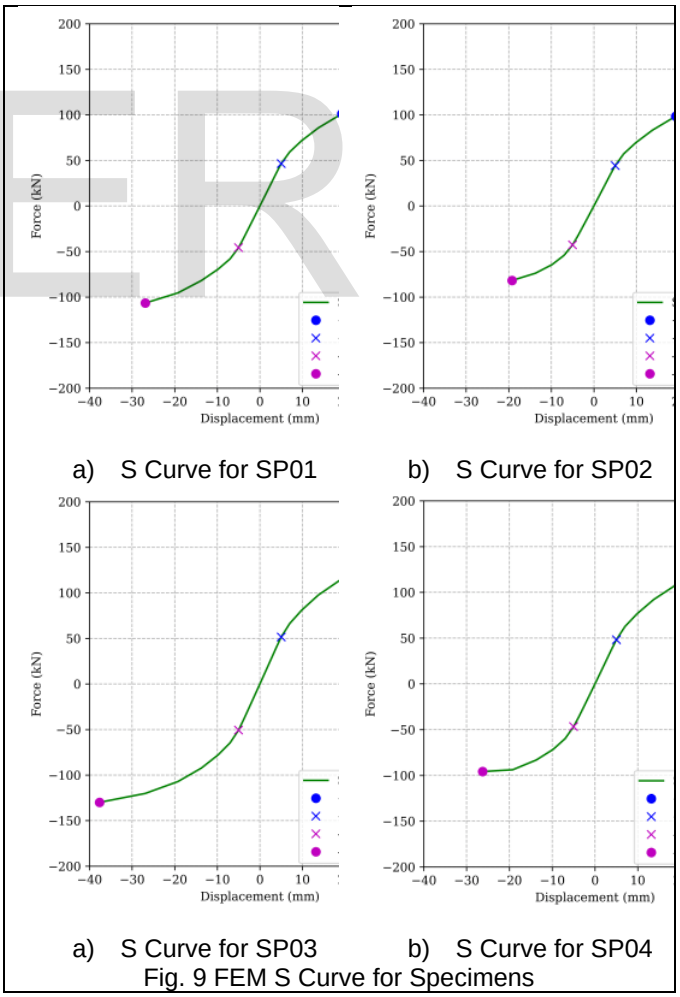

a) S Curve for SP01 b) S Curve for SP02

a) S Curve for SP03 b) S Curve for SP04

Fig. 9 FEM S Curve for Specimens

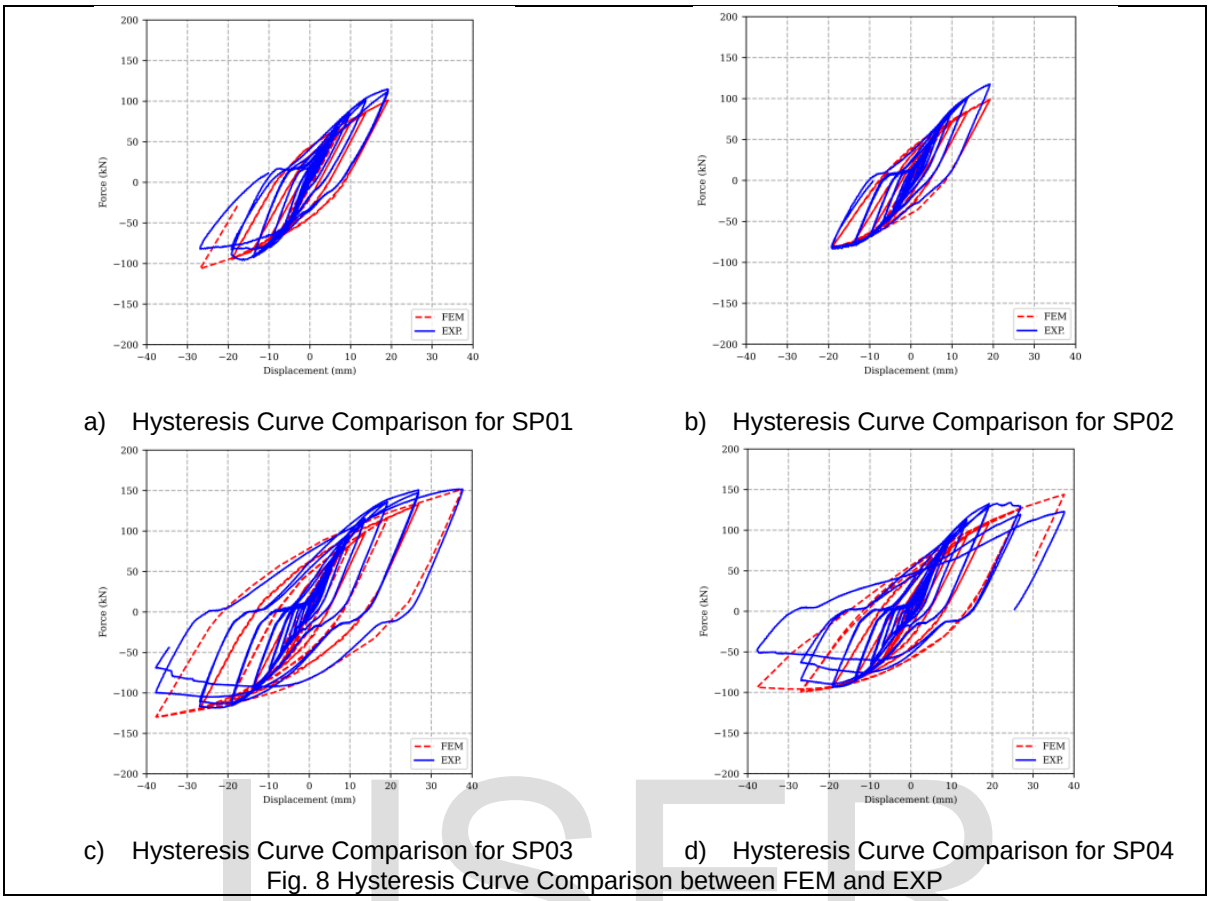

a) Hysteresis Curve Comparison for SP01

b) Hysteresis Curve Comparison for SP02

c) Hysteresis Curve Comparison for SP03

d) Hysteresis Curve Comparison for SP04

Fig. 8 Hysteresis Curve Comparison between FEM and EXP

Table 4 Capacity Comparison for Experiment and FEM

Specimen No.	Experiment		FEM		% diff of P_{u+ve}	% diff of P_{u-ve}
	P_{u+ve}	P_{u-ve}	P_{u+ve}	P_{u-ve}		
SP01	105.58	-89.23	101.13	-106.57	-4.21%	19.43%
SP02	117.80	-83.53	98.72	-81.79	-16.20%	-2.08%
SP03	151.63	-108.91	151.68	-129.95	0.03%	19.31%
SP04	132.50	-95.15	143.95	-95.76	8.64%	0.64%

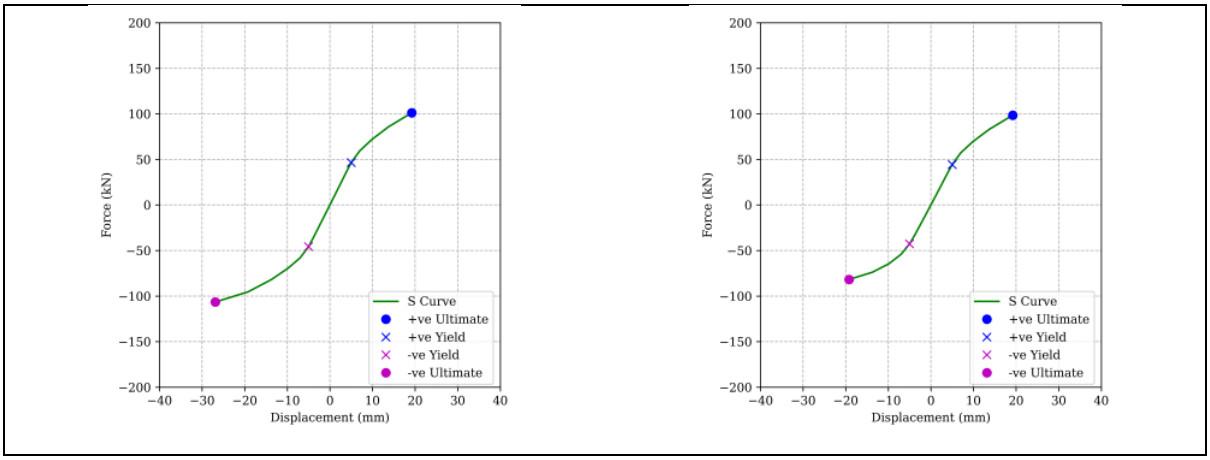

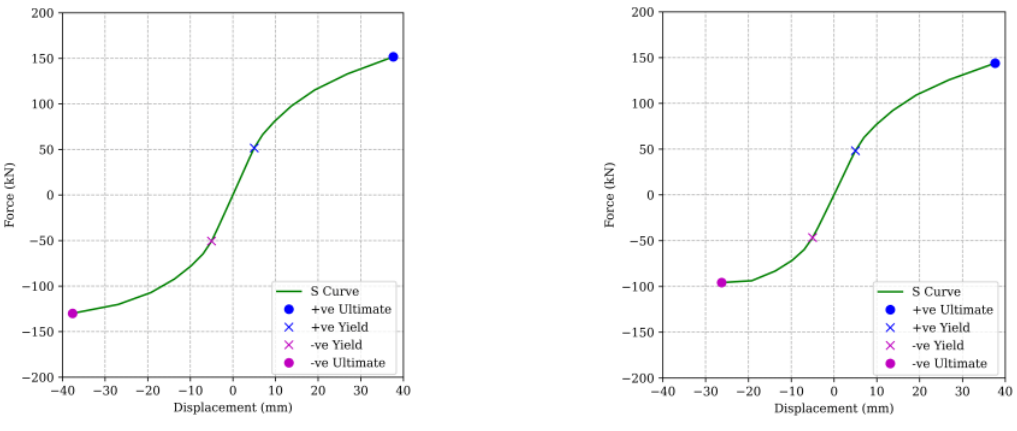

c) S Curve for SP01 d) S Curve for SP02

c) S Curve for SP03 d) S Curve for SP04

Fig. 9 FEM S Curve for Specimens

3.3 Stress Distribution

Distribution of stress and plastic strain leads to predict locations of cracks around brace in connection. SP01 & SP02 had a stress concentration around brace location leading to plastic deformation at crown location as shown in Fig. 10a& b. For other specimen, stiffener reinforced plates redistribute the load along stiffener length, therefore stress concentration was decreased as described in Fig. 10c& d, and so the location of plastic strain and cracks transfer along brace perimeter and stiffener length.

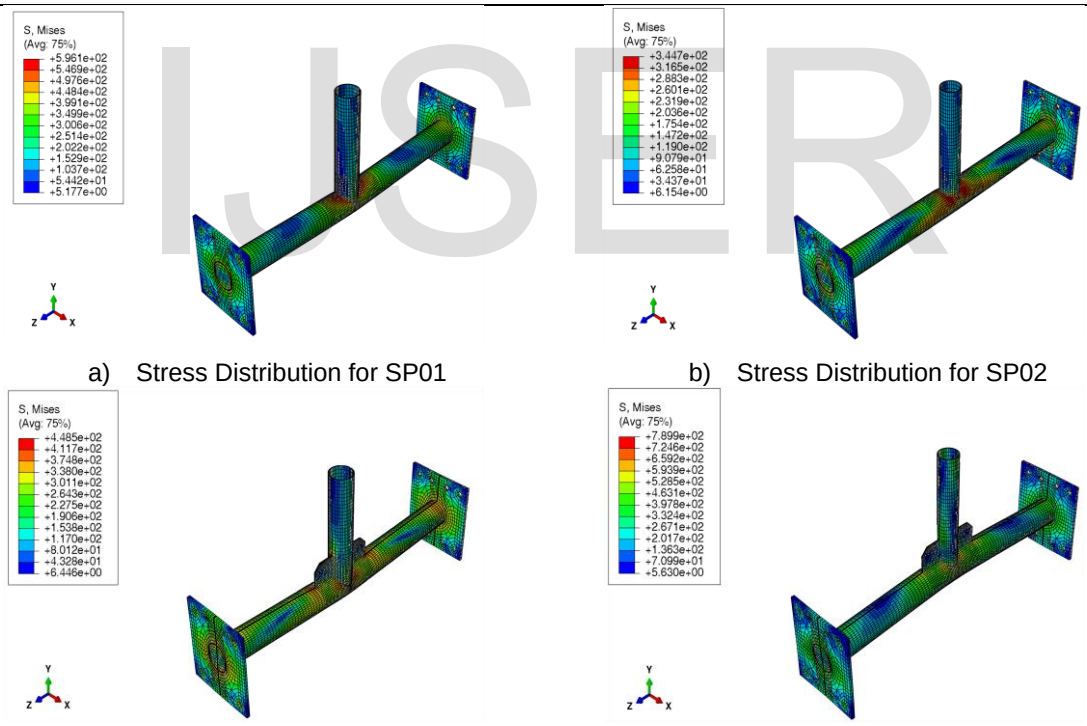

a) Stress Distribution for SP01 b) Stress Distribution for SP02

c) Stress Distribution for SP03 d) Stress Distribution for SP04

Fig. 10 Stress Distribution Around Connection Location

4 Parametric Study

Numerical study was extended with a larger number of FEM to understand the behavior of joints under cyclic load. This research studied joint capacity with change in brace to chord diameter ratio (β= d/D) where d represents brace diameter and D was chord diameter as shown in Fig. 11. Number of models in the parametric study was selected to cover geometry validity as per CIDECT design guide [12] and Chinese Code [13]. Range validity for β was between 0.20 and 1.00, corresponding models and profiles were summarized in Table 5 for unstiffened and stiffened CHS T-joints, T01 and T02, respectively.

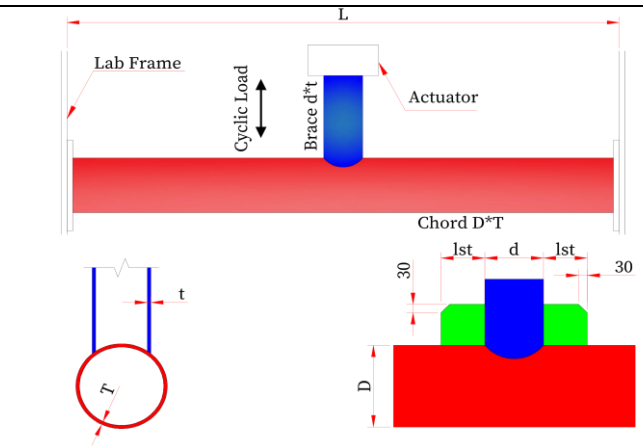

Connection Reinforced with Stiffener

Geometry Parameters:

0.2 < β = d/D < 1.0
D : Chord Diameter
T : Chord Thickness
L : Chord Length
d : Brace Diameter
t : Brace Thickness
lst : Stiffener Pl. Diameter = 0.75*d
tst : Stiffener Pl. Thickness = 6 mm

Fig. 11 Geometry Parameters Definitions

Table 5 Parametric Study Models

Unreinforced Joints	Reinforced Joints	Brace		Chord		Length L (mm)	β
		d (mm)	t (mm)	D (mm)	T (mm)		
T01-01	T02-01	33.7	4	168.3	10	1500	0.20
T01-02	T02-02	42.4	3	168.3	10	1500	0.25
T01-03	T02-03	42.4	4	139.7	8	1500	0.30
T01-04	T02-04	114.3	4	323.9	8	2000	0.35
T01-05	T02-05	177.8	6	355.6	6.3	2500	0.50
T01-06	T02-06	177.8	8	323.9	8	2000	0.55
T01-07	T02-07	244.5	8	323.9	8	2500	0.75
T01-08	T02-08	323.9	8	323.9	8	2000	1.00

Load and displacement versus time data were extracted from history output of FEM, and this data could be analyzed to perform hysteresis curve. Stress distribution and determining location of stress concentration would be plotted from field output of FEM. Analysis of data and comparison among different types would be illustrated in the following sections.

4.1 Hysteresis and S Curve

Behavior of joints have been studied through output comparison variable as positive and negative joint capacity; these variables were evaluated from hysteresis curve. Hysteresis curves were plotted from load displacement data of FEM, and S curves were extracted for each model as shown in Fig. 12.

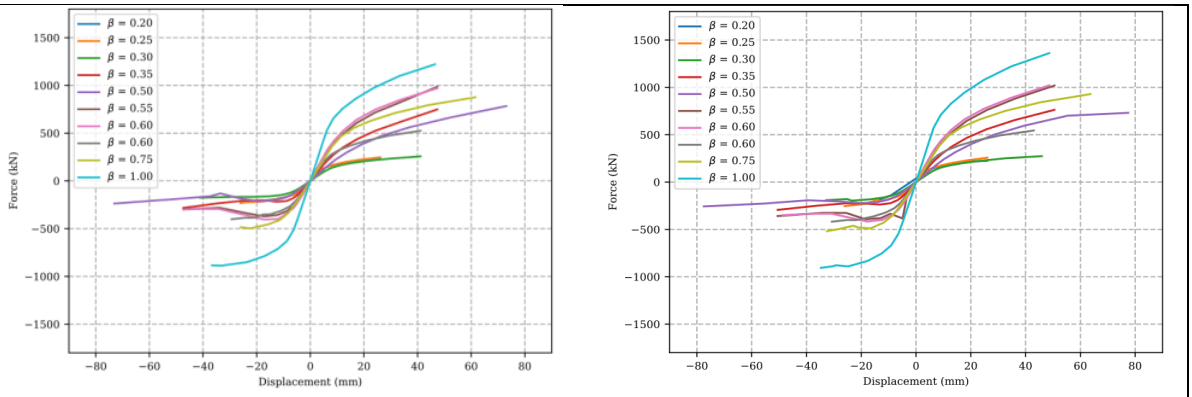

a) S Curve for T01 Models b) S Curve for T02 Models

Fig. 12 S Curve Comparison between Two Types

4.2 Joint Capacity

Joints capacity have extracted from S curve and filtered to can figure out the effect of geometry parameter on positive and negative joint capacity (P_{u+ve} and P_{u-ve}). The data plotted as scatter diagram with dot red color for P_{u+ve} and x red color for P_{u-ve} then smoothed to curve in blue for positive capacity and green for negative capacity. Relation between change in β and joint capacity is described below. Joint capacity was extracted from S curve for the filtered models and listed in Table 6 for all types.

Stiffener did not introduce any joint improvement, except positive capacity increased by 10 % when β > 0.8 as shown in Fig. 13.

Table 6 Positive and Negative Capacities for T01 & T02

β	Positive Capacity (KN)		Negative Capacity (KN)	
	T01	T02	T01	T02
0.20	241.46	224.67	-227.55	-185.60
0.25	246.92	257.60	-226.86	-254.57
0.30	257.25	273.62	-175.88	-196.12
0.35	748.81	762.94	-282.30	-293.74
0.50	784.34	731.09	-365.29	-392.93
0.55	986.46	1019.10	-371.85	-393.60
0.60	970.62	1021.50	-404.61	-417.16
0.75	876.05	929.03	-497.64	-518.60
1.00	1221.50	1361.80	-887.43	-905.65

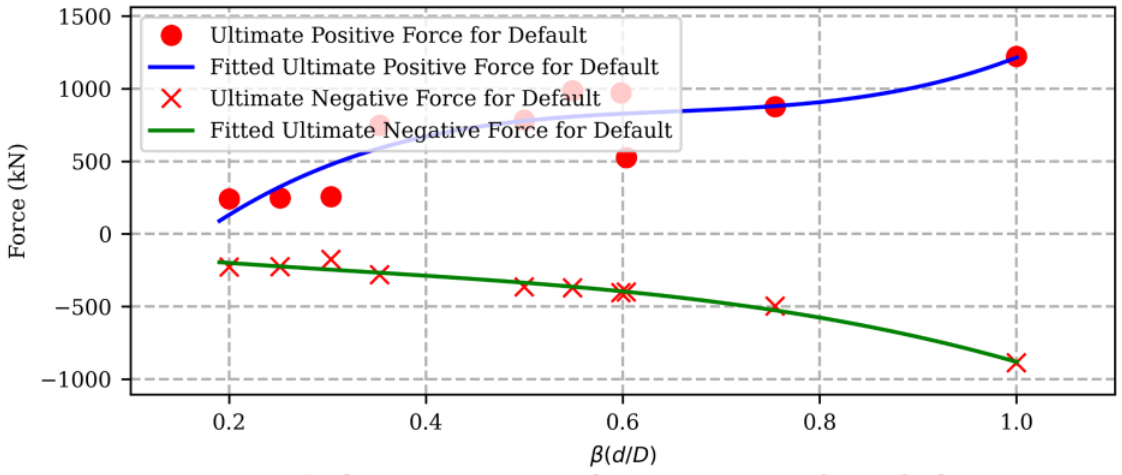

a) Ultimate Positive and Negative Force for Default

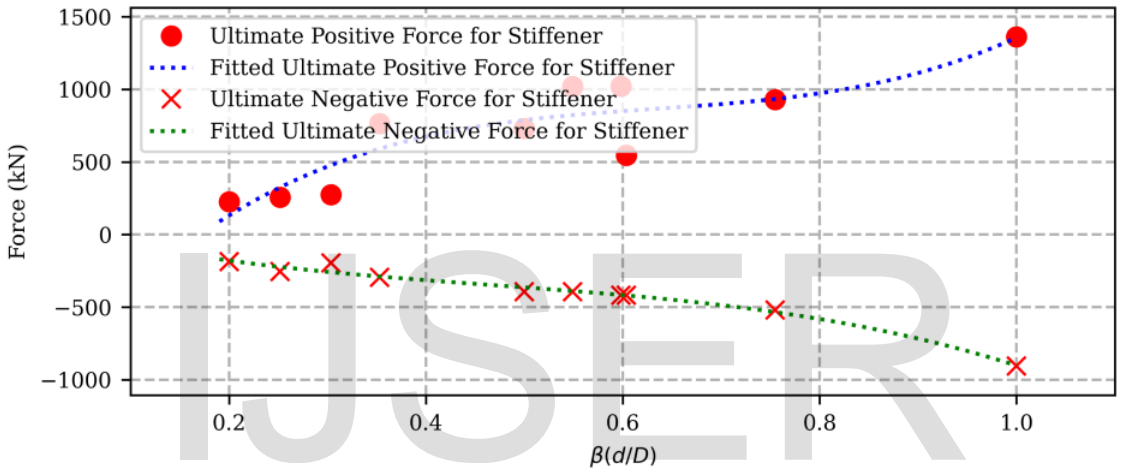

b) Ultimate Positive and Negative Force for Stiffener

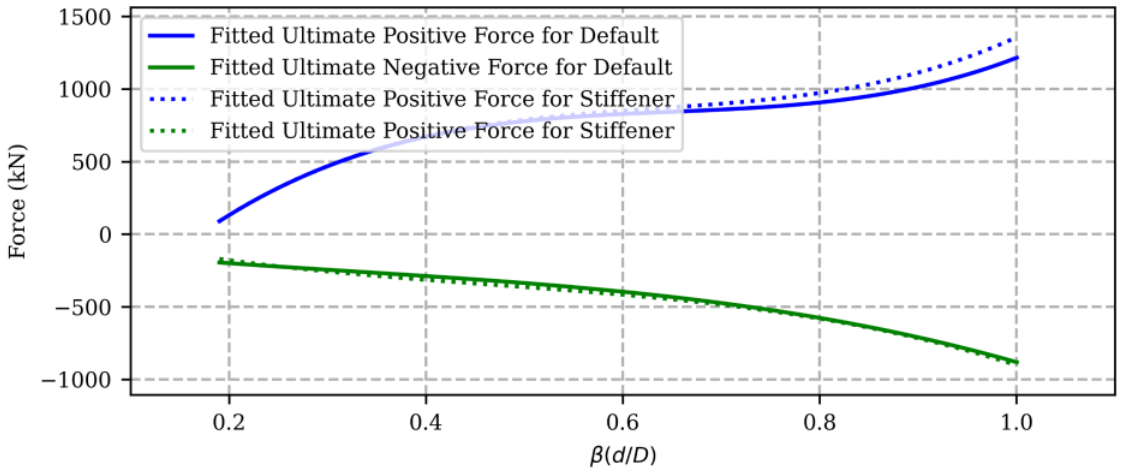

c) Smoothed Ulltimate Forced Comparison between Default & Stiffener

Fig. 13 Capacity Comparison between T01 & T02

For T01, positive capacity can be expressed by fitting (1) and improved positive capacity when using stiffeners is presented by (2).

$$P_{u+ve\_T01} = (19.5\beta^3 - 38.1\beta^2 + 25.9\beta - 3.4)F_y \quad (KN) \quad (1)$$

$$P_{u+ve\_T02} = (20.1\beta^3 - 38.2\beta^2 + 25.6\beta - 3.4)F_y \quad (KN) \quad (2)$$

Negative capacity can be formatted by (3) and (4) for T01 and T02, respectively.

$$P_{u-ve\_T01} = (-3.4\beta^3 + 3.3\beta^2 - 2.4\beta - 0.2)F_y \quad (KN) \quad (3)$$

$$P_{u-ve\_T02} = (-6.0\beta^3 + 8.4\beta^2 - 1.5\beta + 0.3)F_y \quad (KN) \quad (4)$$

4.3 Stress Distribution

Stress distribution could be signs to predict the locations of stress concentration and so cracks propagation locations. Existence of stiffener introduce improvement in stress distribution for all ranges of β as shown in Fig. 14 and Fig. 15. Stiffeners increase the area of load distribution from brace member that allow to decrease stress concentration.

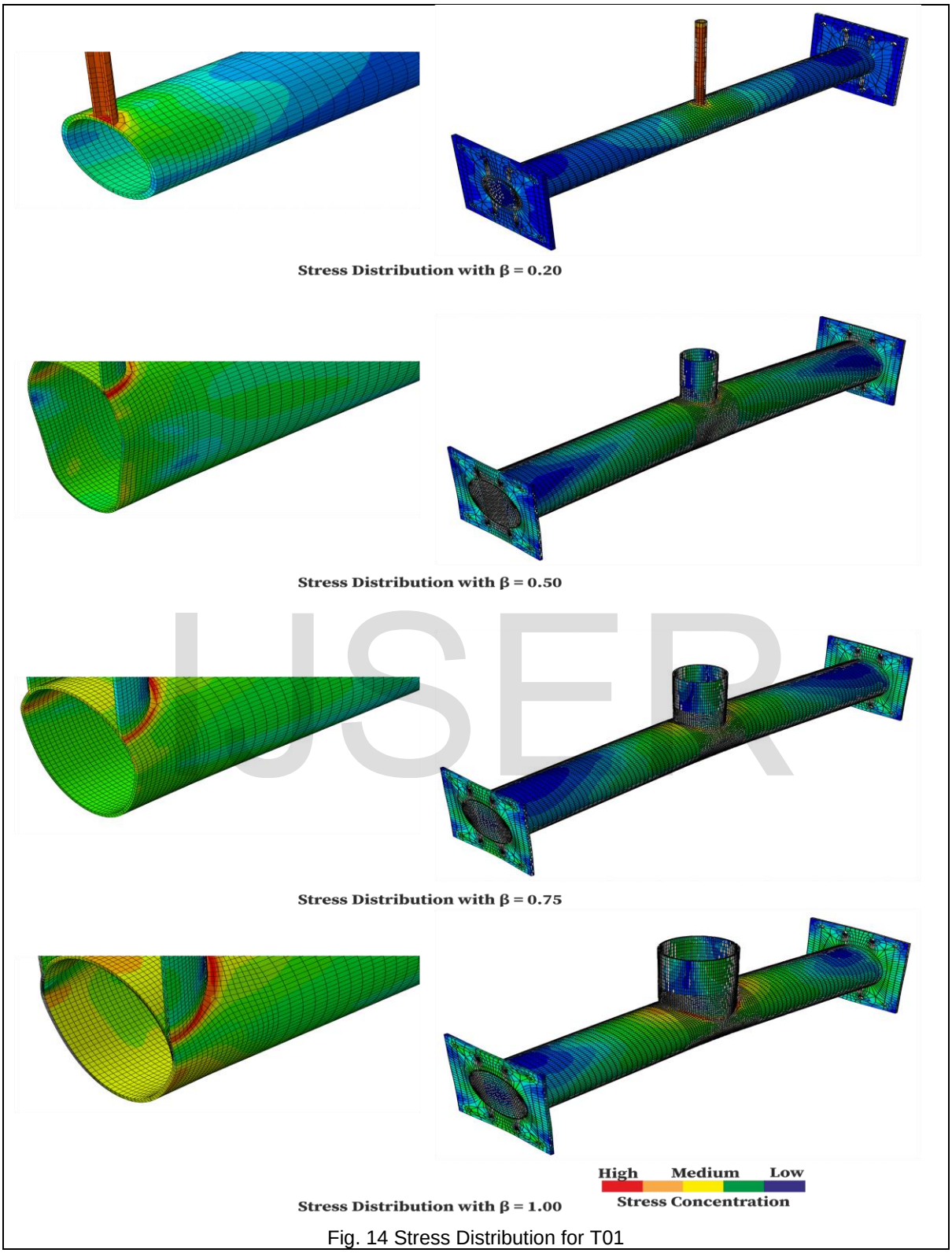

Fig. 14 Stress Distribution for T01

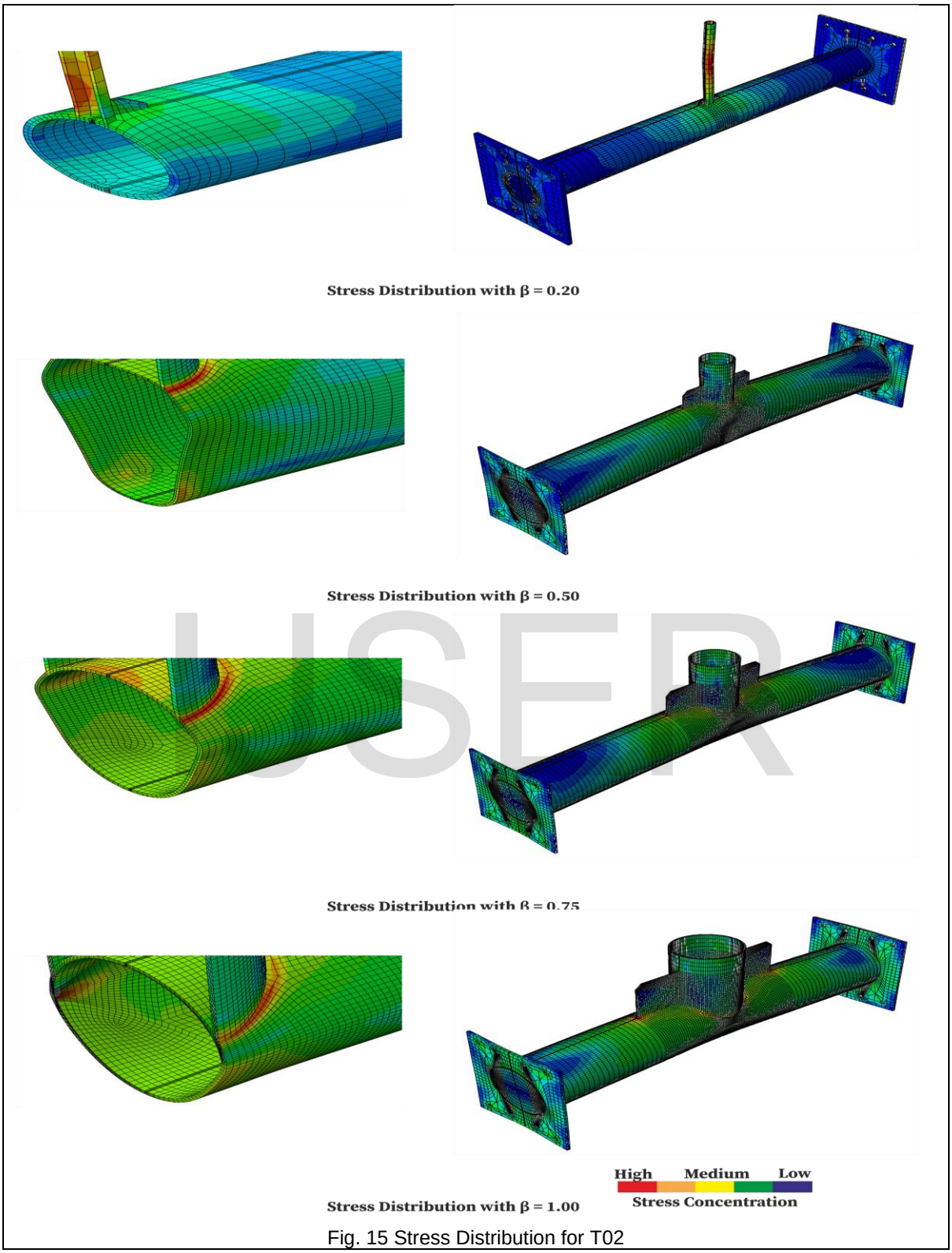

Fig. 15 Stress Distribution for T02

5 Conclusion

CHS joints are usually associated with more complex stresses distribution and therefore become critical locations in tubular structures. Considering the important role of CHS joints, several reinforcing methods have been developed to enhance CHS joints. Stiffener could be used as reinforcing tools for CHS T-joints and most of previous studies investigated the behavior of such joint under static load.

This research studied the effectiveness of reinforcing CHS T-joints with stiffener plate under cyclic load. The study was done through four experimental and numerical specimens subjected to quasi-static cyclic load. Two specimens represented unreinforced T-joints and the others were reinforced with stiffener plate. Hysteretic curves were plotted from load displacement data and S curves were extracted from them. By examining the four full-scale specimens' failure mode, hysteretic curves and energy dissipation, it was found that the enclosed area of the hysteretic curves of the stiffened T-joints is larger than that of the un-stiffened specimens because chord reinforcement improved the joint bearing capacity.

Numerical study results compared with experiment results and they were in favorable agreement. Numerical study was extended to investigate the effectiveness of external stiffener on CHS T-joints with different brace to chord diameter ratio β and fitting equations were extracted to describe this relation.

Although existence of stiffener enhanced connection stress distribution and decreased stress concentration, it was not introducing a remarkable improvement in joint capacity as it was not increase initial stiffness of chord. Positive capacity was enhanced only by 10% and there was unremarkable improvement in negative capacity.

References

[1] Y. Ding, L. Zhu, K. Zhang, Y. Bai, and H. Sun, "CHS X-joints strengthened by external stiffeners under brace axial tension," *Eng. Struct.*, vol. 171, pp. 445–452, 2018.

[2] W. Li, S. Zhang, W. Huo, Y. Bai, and L. Zhu, "Axial compression capacity of steel CHS X-joints strengthened with external stiffeners," *J. Constr. Steel Res.*, vol. 141, pp. 156–166, 2018.

[3] P. G. Melek, S. Gaawan, and A. Osman, "Strengthening Steel CHS X-Joints Subject to Compression by Outer Ring stiffeners," *Int. J. Steel Struct.*, pp. 1–20, 2020.

[4] L. Zhu, Y. Zhao, S. Li, Y. Huang, and L. Ban, "Numerical analysis of the axial strength of CHS T-joints reinforced with external stiffeners," *Thin-Walled Struct.*, vol. 85, pp. 481–488, 2014.

[5] L. Zhu, Q. Song, Y. Bai, Y. Wei, and L. Ma, "Capacity of steel CHS T-Joints strengthened with external stiffeners under axial compression," *Thin-Walled Struct.*, vol. 113, pp. 39–46, 2017.

[6] L. Zhao, L. Zhu, H. Sun, L. Yang, and X. Chen, "Experimental and Numerical Investigation of Axial Tensile Strength of CHS X-Joints Reinforced with External Stiffening Rings," *Int. J. Steel Struct.*, vol. 20, no. 3, pp. 1003–1013, 2020.

[7] V. Abaqus, "6.14 Documentation," *Dassault Syst. Simulia Corp.*, vol. 651, pp. 2–6, 2014.

[8] C. I. Zub, A. Stratan, and D. Dubina, "Calibration of parameters of combined hardening model using tensile tests," 2020.

[9] F. FEMA, "461-Interim protocols for determining seismic performance characteristics of structural and nonstructural components through laboratory testing, Federal Emergency Management Agency (FEMA), Document No," *Redw. City, CA*, 2007.

[10] Y.-B. Shao, T. Li, T. L. Seng, and S.-P. Chiew, "Hysteretic behaviour of square tubular T-joints with chord reinforcement under axial cyclic loading," *J. Constr. Steel Res.*, vol. 67, no. 1, pp. 140–149, 2011.

[11] C. I. Zub, A. Stratan, and D. Dubina, "Calibration of parameters of combined hardening model using tensile tests," *SDSS 2019 - Int. Colloq. Stab. Ductility Steel Struct.*, 2019.

[12] J. Wardenier and J. Wardenier, *Design guide for circular hollow section (CHS) joints under predominantly static loading*. Cidect, 2008.

[13] C. S. GB50017, "Code for design of steel structures," *Ministry of construction of the People's Republic of China*. China Planning Press Beijing, 2003.